International Journal of Hydrogen Energy 78 (2024) 991–1003

Contents lists available at ScienceDirect

International Journal of Hydrogen Energy

journal homepage: www.elsevier.com/locate/he

Comparative energy and exergy analysis of ortho-para hydrogen and non-ortho-para hydrogen conversion in hydrogen liquefaction

Abdurrazzaq Ahmad [a,b], Eni Oko [a,c,*], Alex Ibhadon [a,**]

[a] School of Engineering, University of Hull, HU6 7RX, UK
[b] Department of Chemical Engineering, Federal Polytechnic Mubi, Adamawa State, Nigeria
[c] School of Engineering, Newcastle University, NE1 7RU, UK

ARTICLE INFO

Handling Editor: Dr J Ortiz

Keywords:
Ortho-para-hydrogen conversion
Hydrogen liquefaction
Energy analysis
Exergy analysis
Process simulation

ABSTRACT

This study reports the comparative energy and exergy analysis of ortho-para hydrogen and non-ortho-para hydrogen conversion in hydrogen liquefaction process. Two cases were simulated, case A – hydrogen liquefaction with ortho-parahydrogen conversion and case B – hydrogen liquefaction without ortho-parahydrogen conversion. This is the first study that presents a comparative energy and exergy analysis between such two cases. In this research, a hydrogen liquefaction process was designed adopting cascaded five-stage Brayton refrigeration cycle. The process was simulated in Aspen PLUS. The process used a mixed refrigerant (of liquefied natural gas) refrigeration cycle to precool the gaseous hydrogen feed from 26 °C temperature to −192 °C temperature, and mixed refrigerant (of nelium) was subsequently used to further deep-cool the the hydrogen stream from −192 °C temperature to −245.99 °C temperature in the cryogenic section of the process. Liquefaction was achieved by expanding the hydrogen through Joule-Thomson valve at −248.37 °C and 1 bar. The simulated results of the two cases showed the specific energy consumption of case A to be 8.45 kWhr/kg_{LH}, and that of case B to be 15.65 kWhr/kg_{LH} respectively. The results also indicated a total exergy efficiency of 92.42% in case A and 87.18% in case B. The research results showed that the hydrogen liquefaction designed with configuration of ortho-parahydrogen conversion has better performance indicators than the liquefaction without ortho-parahydrogen conversion. Therefore, hydrogen liquefaction with ortho-parahydrogen conversion can be considered in the design and development of new hydrogen liquefaction plants. Process optimization is recommended to further enhance the specific energy consumption and exergy efficiency of both processes.

Nomenclature

A, B	Study case identifier (e.g., Case A)
SEC	Specific Energy Consumption
COP	Coefficient of Performance
OPHC	Ortho - Parahydrogen Conversion
GH	Gaseous Hydrogen
MR	Mixed Refrigerants
HEX	Heat Exchanger
BO	Boil off
T-H	Temperature – Enthalpy
p-H_2	Parahydrogen
o-H_2	Orthohydrogen
K_{eq}	Equilibrium constant
T	Temperature
P	Pressure
P_{re}	Reference pressure
W_{cp}	Compressor duty (kW)
W_{tb}	Expander/Turbine duty (kW)
Q_{hex}	Heat exchanger duty (KW)
Q_{col}	Cooler duty (kW)
H	Enthalpy flow (kW)
W_{total}	Total work (kW)
Ex	Exergy (kW)
Ex_{dest}	Exergy destruction (kW)
I	Equipment Exergy efficiency (%)
CMP/cp	Compressor
TRB/tb	Expander/Turbine
PMP/pp	Pump
COL/col	Cooler
SEP/sp	Separator

(*continued on next column*)

(*continued*)

(*continued on next page*)

* Corresponding author. School of Engineering, University of Hull, HU6 7RX, UK
** Corresponding author.
E-mail addresses: eni.oko@newcastle.ac.uk (E. Oko), a.o.Ibhadon@hull.ac.uk (A. Ibhadon).

https://doi.org/10.1016/j.ijhydene.2024.06.368
Received 21 January 2024; Received in revised form 2 May 2024; Accepted 26 June 2024
Available online 2 July 2024

(*continued*)

MIX/mx	Mixer
VAL/val	Valve
m_{in}	Stream mass flow rate in (kg/sec)
m_{ou}	Stream mass flow rate out (kg/sec)
η	System total exergy efficiency (%)
R14	Tetrafluoromethane
FM	First mixed refrigerant stream
SM	Second mixed refrigerant stream

1. Introduction

The increasing global need for eco-friendly and renewable energy sources has accelerated research efforts aimed at efficient hydrogen production and storage technologies [1]. Hydrogen, being a versatile and environmentally friendly energy carrier, has gained significant attention as a potential solution for reducing carbon emissions and mitigating climate change [2]. In the race to secure clean energy for the future, several storage strategies for hydrogen like compressed hydrogen, liquid hydrogen, and metal hydrides have been studied [3–5].

The choice of the optimal storage mechanism for hydrogen is dependent upon various factors, such as the scale of storage, transportation distances involved, and the intended application of the hydrogen [6]. In this regard, liquid hydrogen is considered a highly promising option for large-scale hydrogen storage and transportation due to its significant advantages. Specifically, at a temperature of −253.2 °C and a pressure of 1.0 bar, liquid hydrogen exhibits a high volumetric density of 71.3 kg/cm^3 [7], not only that, but hydrogen in liquid form also possesses high energy density compared to gaseous hydrogen [4,8]. These encouraging properties of liquid hydrogen and the success story recorded by liquefied natural gas attracted attention to hydrogen liquefaction [9]. Harnessing the full potential of liquid hydrogen is its liquefaction, as it enables its efficient storage and transportation [10]. As a result, the liquefaction of hydrogen plays a vital role in facilitating the widespread utilization of hydrogen [11]. Hydrogen liquefaction process is carried out in three main stages that include: precooling (from 25 °C to −193 °C), cryogenic cooling that involves ortho to parahydrogen conversion process (from −193 °C to −243 °C), and expansion/liquefaction (from −224 °C to −253 °C) [9]. Different methods for hydrogen liquefaction have been extensively described and analysed in other literature sources [4].

Recent research has identified various approaches to enhance the performance of hydrogen liquefaction [12]. One of the integral components of hydrogen liquefaction and a major determinant of the specific energy consumption (SEC) is associated with the molecular state of hydrogen [13]. Hydrogen as a diatomic molecule consists of two distinct isomers in the form of ortho- and para-modifications. This modification is expected to be present in all diatomic molecules of identical atoms with nuclear spin [14]. The hydrogen isomers are determined by the spin orientation of their nuclei, resulting in slight differences in their properties with ortho hydrogen having nuclei spin in one direction, and para hydrogen having nuclei spin oppositely (Fig. 1). These hydrogen isomers exhibit differing rotational energies, with ortho hydrogen existing in an excited state with higher energy levels than para hydrogen. Consequently, the equilibrium between these states is temperature-dependent, favouring a higher percentage of para hydrogen as temperatures approach −253 °C [15].

As the equilibrium concentration of para hydrogen and the heat released during conversion are temperature dependent, at room temperature, the equilibrium mixture of hydrogen comprises 75% ortho hydrogen and 25% para hydrogen [17]. Ortho hydrogen having a higher energy state undergoes spontaneous exothermic conversion, albeit sluggish into para hydrogen. At temperatures reaching −253 °C, the concentration of para hydrogen significantly rises to over 98% [4]. Therefore, if hydrogen is stored without undergoing catalytic conversion of the ortho hydrogen to para hydrogen during the liquefaction process, up to 50% of the liquefied hydrogen could evaporate within a span of 10 days requiring re-liquefication [17]. Consequently, the integration of catalytic ortho-para hydrogen conversion (OPHC) has become an essential component in hydrogen liquefaction processes [18]. This incorporation will enable the transformation of ortho hydrogen into para hydrogen, preventing excessive evaporation, and ensuring the stability of the liquid hydrogen [19]. However, the incorporation of the catalytic conversion introduces additional energy penalty to the process.

Current research in the literatures extensively explored hydrogen liquefaction processes involving OPHC [12]. OPHC is recognized for its role in enhancing hydrogen's thermodynamic behaviour during liquefaction [20]. However, there is no assessment of hydrogen liquefaction without OPCH. This observation was emphasised by Raiz et al., [9]. Research by Teng et al. attempted to address this issue but was limited only to hydrogen liquefaction with catalytic OPHC. The work analysed three different models of hydrogen liquefaction with catalytic OPHC based on the three fundamental OPHC methods, i.e., isothermal, adiabatic and continuous conversion methods. Their comparative analysis focused on parameters such as temperature distribution, conversion-heat-associated exergy, and specific energy consumption (SEC). Results showed that the continuous conversion method has the lowest SEC value at 11.38 kWh/kgLH2, representing a notable decrease of 21.8% and 28.7% compared to the adiabatic and isothermal methods, respectively. Moreover, exergy consumption related to dissipating the conversion heat was found to be the lowest in the continuous conversion model (139.54 kW), followed by the adiabatic and isothermal conversion methods, with values of 174.94 kW and 273.90 kW, respectively [21]. The aforementioned observation necessitated the need to investigate aspects of hydrogen liquefaction without OPHC to ensure a comprehensive understanding of the implication of OPHC on energy and exergy of hydrogen liquefaction systems. Therefore, the objective of this research is to assess the energy and exergy analysis of two hydrogen liquefaction systems (i.e., OPHC and non-OPHC systems).

To do so, the study evaluated and compared the energy and exergy aspects of the two processes. By conducting this analysis, the study

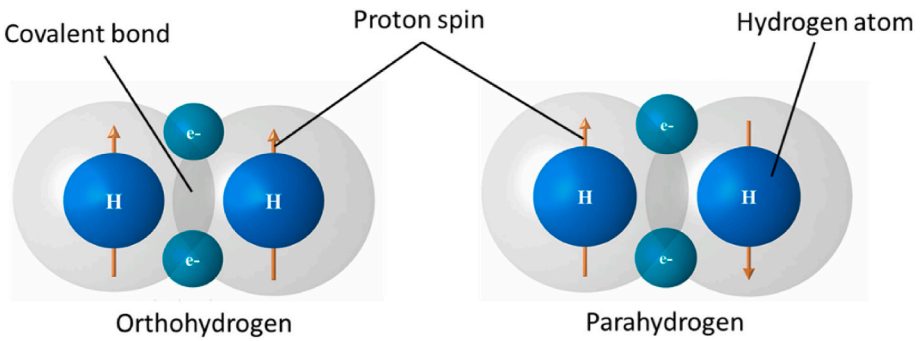

Fig. 1. Hydrogen spin isomers [16].

aimed to understand the implications of incorporating OPHC versus non-OPHC in terms of energy efficiency (energy analysis that involves assessing the energy inputs, outputs, and transformations within the hydrogen liquefaction process), exergy losses (exergy analysis that considered the quality of energy and potential for useful work), and overall system performance which will provide insights into the necessity and impact of OPHC on the hydrogen liquefaction system, enabling a better understanding of its benefits and potential drawbacks. This will lead to better decision-making regarding the adoption of OPHC in practical hydrogen liquefaction applications.

2. Process description and model development

2.1. Process description

Fig. 1 shows the process flow diagram of the integrated system of hydrogen liquefaction comprising components for compression, precooling and cryogenic liquefaction. Aspen PLUS software tool was used to simulate the process. The detailed description of the two scenarios referred to as Case A (hydrogen liquefaction model with fully incorporated reactor operators of OPHC) and Case B (hydrogen liquefaction model without the chemistry operators of OPHC) were considered in the study. The hydrogen liquefaction process was modelled based on the continuous conversion method. In the process, feed hydrogen gas, H0 was compressed to a pressure of 21 bar. In the first step of the precooling cycle, the compressed hydrogen stream, H1, is introduced into HX1. During this stage, H1 undergoes heat exchange with a cold stream, W1, resulting in a temperature drop of H1 to 26 °C. The second stage of the precooling was applied using the first mixed refrigerant consisting of methane, ethane butane, nitrogen propane pentane, r-14, and ethylene (see Table 2 for mole composition) for the completion of the precooling cycle to subsequently attain a temperature of −192 °C through HX2 to HX4.

Eventually, stream H5 from HX4 was further cooled in a cryogenic cycle (second refrigeration cycle) using a second mixed refrigerant composed of Nelium (helium and neon, see Table 2). Under this process, stream H5 was passed through a series of heat exchangers that included HX5, HX6, HX7, HX8, and HX9 which dropped the temperature to −244.13 °C to obtain stream H10. The step-by-step cryogenic cooling was achieved using four cascaded Helium-Brayton cycles connected to the five heat exchangers carrying the hydrogen streams. The feed hydrogen is ultimately throttled using a Joule-Thomson valve, V2, to obtain liquified hydrogen (stream H11 at 245.99 °C) as the product.

However, in case B, the presence of gaseous phase hydrogen due to boil-off during liquefaction necessitated the separation of stream H11 through flashing in a separator. This separation aimed to isolate the liquid phase of hydrogen from its gas phase. The separated gaseous hydrogen was subsequently recycled, for reintegration into the liquefaction as stream H13 through to stream H15 to meet Stream H5 at MIX6 (see Fig. 3).

Maintaining a similar configuration in both cases allowed for the comparative investigation of the impacts of various energy factors on the hydrogen liquefaction process. By comparing the performance, and energy efficiency of these models, valuable insights can be gained to inform the selection of a practical hydrogen liquefaction model.

2.1.1. For case A

See Fig. 2. The hydrogen feed subsequently flows through a sequence of cryogenic stage heat exchangers (HX5 - HX9) equipped with the kinetics of Fe_2O_3 catalysed ortho-parahydrogen conversion.

2.1.2. Reaction type and stoichiometry

Technically, achieving ortho-para conversion involves loading the hydrogen side of the heat exchangers with a suitable catalyst, promoting equilibrium and dissociation reactions [4]. The process occurs simultaneously and unfolds in the following manner:

$$o - H_2 \rightleftharpoons p - H_2 \tag{1}$$

$$H_2 \rightleftharpoons p - H_2 \tag{2}$$

the equilibrium constant:

$$\ln k_{eq} = A + B\left(T^{-1}\right) + C\ln(T) + D(T) + E\left(\frac{P - P_{ref}}{P_{ref}}\right) \tag{3}$$

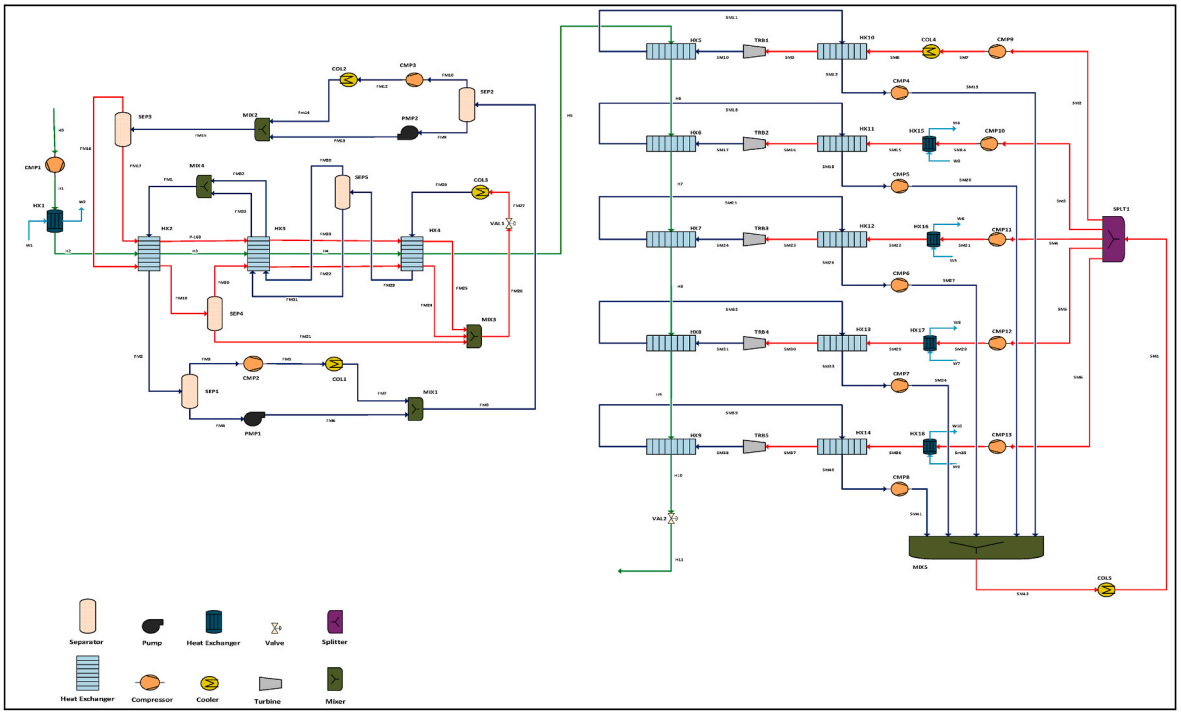

Fig. 2. Integrated system of the Case A model.

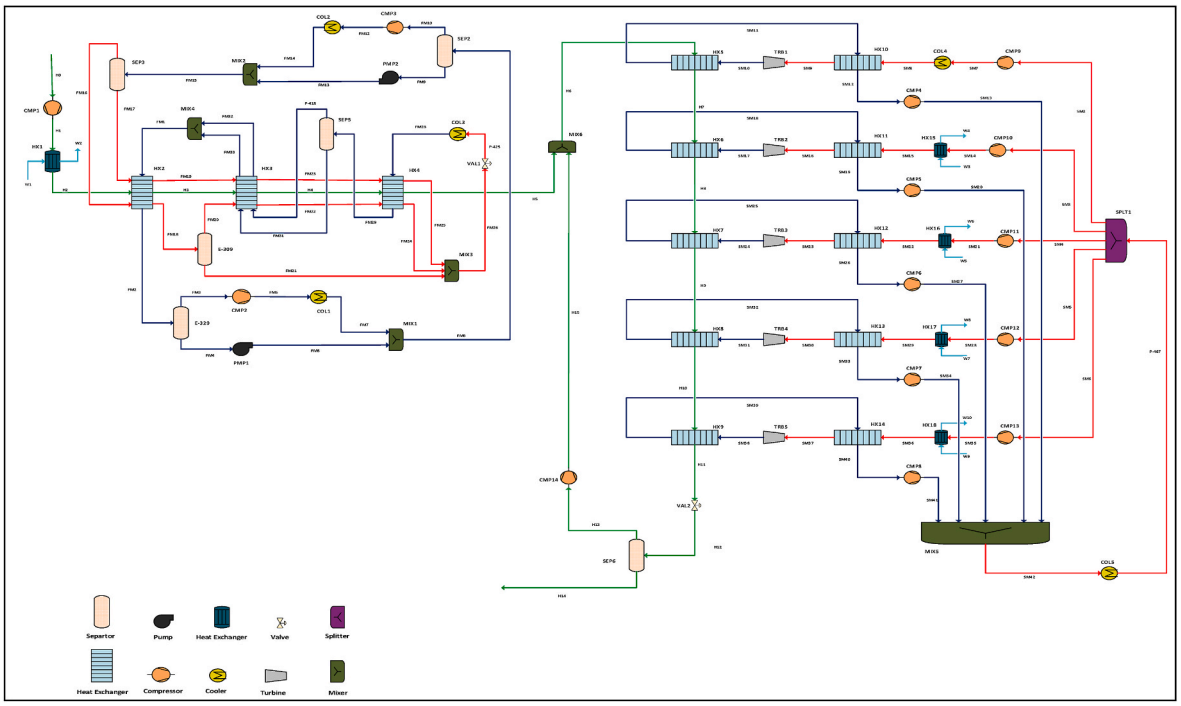

Fig. 3. Integrated system of the Case B model.

where, A, B, C, D, and E values are 5.18192049, −195, −0.61661082, 0.000318 and 0 respectively, while T, P and P_{ref} are the temperature of the hydrogen in degrees Celsius, pressure of the hydrogen and reference pressure of the simulated model in bars respectively [24,25].

Therefore, equation (3) becomes.

$$\ln k_{eq} = 5.18192049 - 195\left(T^{-1}\right) - 0.61661082\ln(T) + 0.000318(T) \tag{4}$$

2.1.3. For case B

See Fig. 3. The hydrogen is directed through a sequence of cryogenic refrigeration heat exchangers (HX5 - HX9) without the presence of ortho-parahydrogen conversion.

The dependence of ortho hydrogen and para hydrogen concentration on temperature in a hydrogen sample was calculated using the following equation [19].

$$\frac{y_{p-H_2}}{y_{o-H_2}} = \frac{1}{3}\left\{\frac{1+5[\exp(-6B/T)]}{3[\exp(-2B/T)]+7[\exp(-12B/T)]}\right\} \tag{5}$$

where:

$$B = \frac{h_p{}^2}{8\pi^2 I_T k_B}86.2K \tag{6}$$

$h_p = 6.626\text{x}10^{-34}$ Js

$k_B = 1.3806\text{x}10^{-23}$ JK^{-1}

$I_T = 4.67\text{x}10^{-48}kgm^2$

T = Temperature (K)

y = concentration $\left(\text{mol mol}^{-1}\right)$

2.2. Choice of refrigerants

In the modelling of the hydrogen liquefaction system, two distinct MRs are used. The first MR is composed of the eight-component mixture (methane, ethane, butane, nitrogen, propane, pentane, R14, and ethylene) [26,27]. For the second MR, Nelium was selected. Nelium, a mixture of helium and neon gases, has been identified to be effective in optimizing the liquefaction process of hydrogen [28].

2.3. Modelling

To evaluate the impact of OPHC on the SEC of the hydrogen liquefaction system, a benchmark process of 1 kmol/h of hydrogen gas was used [22]. Tables 1 and 2 show the conditions of feed streams and compositions with their respective mole fractions used in the models. The equipment specifications and stream conditions were presented in Tables S1 and S2 (see supporting article).

The process relies on a Brayton cycle that incorporates mixed refrigerant precooling and cryogenic refrigeration. By comparing the outcomes of hydrogen liquefaction with and without catalytic OPHC, the influence of OPHC on SEC was effectively assessed.

The liquefaction processes of hydrogen were simulated using Aspen Plus, considering both scenarios with and without ortho-parahydrogen conversion. The simulation used the Peng-Robinson equation of state. To simplify the simulation analysis, several assumptions as follows were made [11]:

Table 1
Hydrogen, water, first and second mixed refrigerant feed conditions.

Quantity	Units	Hydrogen Feed	Cooling feed		
			Water	First MR	Second MR
Temperature	C	25	25	−58	24
Pressure	Bar	4	1	2	2
Average MW	mol/kg	2.01588	18.01528	41.04578	5.65266
Mass Flows	kg/sec	0.0005	0.005	0.01140	0.00157
Volume Flow	m^3/sec	0.00172	3.88348 × 10^{-6}	0.00166	0.00343

Table 2
Feed compositions of hydrogen, water and the two mixed refrigerants [22].

Stream	Component	Mole fraction (%)
Hydrogen feed	Hydrogen	1
First MR	Methane	0.17
	Ethane	0.07
	Butane	0.02
	Nitrogen	0.17
	Propane	0.18
	Pentane	0.15
	R-14	0.08
	Ethylene	0.16
Second MR	Helium	0.898
	Neon	0.102
Water	Water	1

i. Heat loss in heat exchangers, pipelines, and valves is not taken into consideration.
ii. The pressure drop on the cold fluid side (refrigeration cycle) is not accounted for.
iii. All operations were simulated assuming steady-state conditions.
iv. Negligible losses occur in the mechanical transmission of compressors and expanders.
v. Mixed refrigerants were utilized as the working fluid in the refrigeration cycles.

These assumptions were derived from the typical properties observed in a steady-state hydrogen liquefaction process [23]. The purpose of these assumptions is to simplify the simulation process and reduce computational complexity. It was believed that these assumptions were valid. Moreover, as these assumptions remain consistent for both investigated cases, their impact on the processes, with or without the conversion method, will be minimal. In other words, while the assumption may influence the absolute values of the results, they are unlikely to affect the main conclusion.

2.4. Comparative analyses

2.4.1. Energy and exergy analysis

To assess the thermodynamic performance of the systems, calculations and balance equations were applied to evaluate parameters such as outlet enthalpies, and exergies, ensuring a coherent and logical analysis. Fig. 4 shows the adopted procedure for the analysis. Table 2 presents the primary balance equations employed in the systematic analyses [11,24]. These equations cover a range of essential aspects, including mass conservation, energy conservation, and exergy calculations, all specifically tailored to the various streams under examination as such they underpin the rigorous analysis of the system.

In thermodynamic processes, SEC, and coefficient of performance (COP) are widely recognized as significant indicators of energy performance [25]. COP, specifically employed to evaluate the effectiveness of refrigeration cycles, quantifies the ratio of absorbed heat at low temperatures to the net power consumed by the process. On the other hand, SEC, like the COP, quantifies the overall energy consumption in the process in relation to the mass flow rate of the production. In the context of the large-scale hydrogen liquefaction process, the expressions for SEC [22,24] and COP [26] were as follows:

$$SEC = \frac{W_{net}}{\dot{m}_{feed,GH} \times 3600} = \frac{\sum W_{cp} - \sum W_{ep}}{\dot{m}_{LH}} \tag{4}$$

$$COP = \frac{\dot{m}_{LH}\left(h_{feed,GH} - h_{product,LH}\right)}{W_{total}} \tag{5}$$

3. Results and discussion

3.1. Conversion of orthohydrogen to parahydrogen

In a hydrogen liquefaction process analysis, it is important to note the progress of ortho-parahydrogen conversion within the heat exchangers. Table 4 shows the conversion mole fraction of orthohydrogen and parahydrogen stream-by-stream as the feed gaseous hydrogen undergoes liquefaction. Furthermore, the process was able to achieve 97.79% parahydrogen in case A.

3.2. Energy performance analyses

Liquefaction processes require a significant amount of energy because the compression cycle in the refrigeration cycle consumes a large amount of energy. The energy consumption is mainly affected by the suction and discharge pressures, as well as the specific composition of the refrigerant employed in the cycle [27,30]. The energy input and output variations of the equipment in the two cases as simulated are analysed.

Based on the energy assessment conducted for the simulated process, Fig. 5 represents the energy consumption, production, and transfer in the three major equipment of each cycle i.e., the precooling, cooling, and liquefaction within the hydrogen liquefaction system.

The analysis demonstrates that in both Case A and B, the cooling-liquefaction (C-L) compressors account for a significant portion of the energy demand, with duty requirements of 87.17 kW and 123.72 kW, respectively. This is primarily attributed to the substantial energy required to achieve the extremely low temperatures necessary for the process and the high number of compressors present in the cycle. However, Case A exhibits a more efficient energy utilization, with a 36.55 kW reduction in energy input compared to Case B.

Table 3
Basic energy and exergy equations for the equipment of the modelled hydrogen liquefaction system.

Equipment	Energy equation	Exergy destruction	Exergy efficiency	Reference
Compressor	$W_{cp} = \dot{m}_{out,cp}h_{out,cp} - \dot{m}_{in,cp}h_{in,cp}$	$I_{cp} = \dot{m}_{in,cp}ex_{in,cp} - \dot{m}_{out,cp}ex_{out,cp} + W_{cp}$	$\eta_{cp} = 1 - (1/W)$	[27,28]
Expander	$W_{ep} = \dot{m}_{out,ep}h_{out,ep} - \dot{m}_{in,ep}h_{in,ep}$	$I_{ep} = \dot{m}_{in,ep}ex_{in,ep} - \dot{m}_{out,ep}ex_{out,ep} - W_{ep}$	$\eta_{ep} = 1 - [1/(ex_{in} - ex_{out})]$	[27,28]
Heat exchanger	$Q_{hx} = \sum \dot{m}_{j,hx}\left(h_{out,j} - h_{in,j}\right)$	$I_{hx} = \sum \dot{m}_{j,hx}\left(ex_{in,j} - ex_{out,j}\right)$	$\eta_{hx} = \sum ex_{out}/\sum ex_{in}$	[27,28]
Pump	$W_{pp} = \dot{m}_{out,pp}h_{out,pp} - \dot{m}_{in,pp}h_{in,pp}$	$I_{pp} = \dot{m}_{in,pp}ex_{in,pp} - \dot{m}_{out,pp}ex_{out,pp} + W_{pp}$	$\eta_{pp} = 1 - (1/W)$	[27,28]
Cooler	$Q_{col} = \dot{m}_{out,col}h_{out,col} - \dot{m}_{in,col}h_{in,col}$	$I_{col} = \dot{m}_{in,col}ex_{in,col} - \dot{m}_{out,col}ex_{out,col}$	$\eta_{cl} = 1 - \left[1/\sum\left(ex_{in} + ex_{in,air}\right)\right]$	[27,28]
Separator	$\dot{m}_{in,j}h_{in,j} = \sum \dot{m}_{out,j}h_{out,j}$	$I_{sp} = \dot{m}_{in,j}ex_{in,j} - \sum \dot{m}_{out,j}ex_{out,j}$	$\eta_{hx} = \sum ex_{out}/ex_{in}$	[27,28]
Mixer	$\sum \dot{m}_{in,j}h_{in,j} = \dot{m}_{out,j}h_{out,j}$	$I_{mx} = T_o\left(\dot{m}_{out,j}h_{out,j} - \sum \dot{m}_{in,j}h_{in,j}\right)$	$\eta_{mx} = 1 - (1/\sum ex_{in})$	[27,28]
Valve	$h_{in,vl} = h_{out,vl}$	$I_{vl} = \dot{m}_{in,vl}ex_{in,vl} - \dot{m}_{out,vl}ex_{out,vl}$	$\eta_{vl} = 1 - (1/\sum ex_{in})$	[27,28]
Physical exergy		$Ex_{phy} = (h - h_o) - T_o(s - s_o)$		[29]
Chemical exergy		$Ex_{chm} = \sum x_j ex_{o,j}^{chm} + RT_o \sum x_j \ln x_j$		[26]
System Exergy efficiency		$\eta_{ex} = \left(ex_{product,LH} - ex_{feed,GH}\right)/W_{total}$		[28]

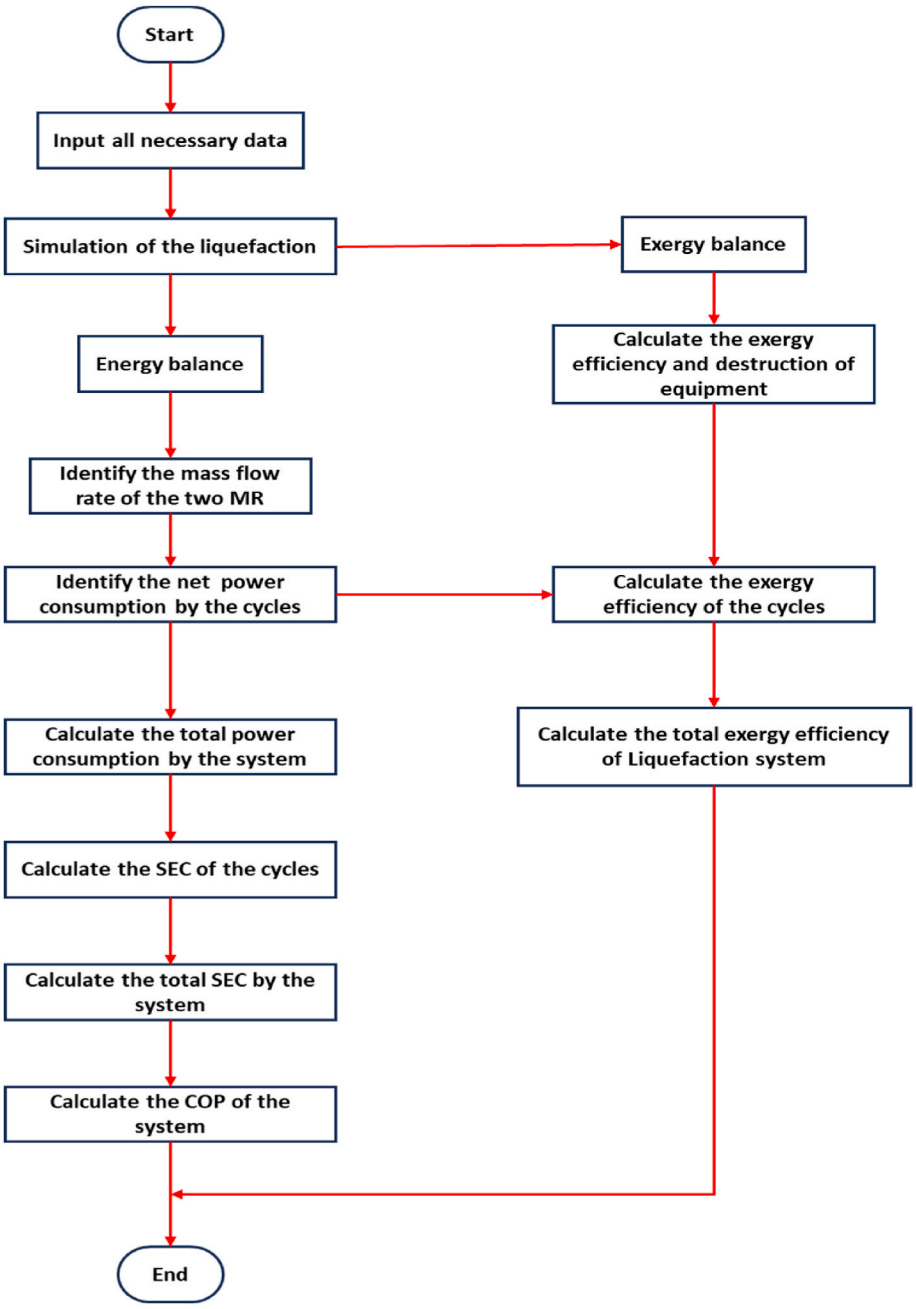

Fig. 4. Methodology adopted for energy and exergy analyses in the comparative study.

This observation replicates itself in C-L coolers, with the coolers accounting for 76.29 kW and 114.69 kW in Case A and B, respectively. This indicates that case A is favourable with 38 kW duty reduction.

Furthermore, from Fig. 5, the precooling (P–C) cycles of the model cases showed little or no differences in cycle comparisons. However, the energy generated by the expanders in the C-L cycle of the model cases showed that Case A generated higher energy of 5.90 kW for its system than Case B with 4.31 kW.

Based on the energy assessment (in terms of thermal energy) conducted for the simulated processes, Fig. 6 represents the energy-consuming and producing units within the model. The analysis demonstrates that in both Case A and B, the compressors account for a significant portion of the energy demand, with duty percentages of 40% and 40.1%, respectively. This is primarily attributed to the substantial energy required to achieve the extremely low temperatures necessary for the process, especially in the C-L cycle. However, Case A exhibits a slightly more efficient energy utilization, with a 0.1% reduction in energy input compared to Case B.

Regarding the utilization of the coolers, Fig. 6 indicates that they represent the second-highest thermal energy consumers after the compressors. Collectively, these coolers account for 35.4% of the total energy requirements for the system in Case A and 37.5% in Case B, respectively. The coolers predominantly function within the precooling phase of the liquefaction process. Therefore, the accumulated energy input in this subsection resulted from the elevated temperatures generated during the compression of gaseous hydrogen (GH) before liquefaction.

In this model, the heat exchangers (Mult-HEX) were configured with a minimum temperature approach of 1 °C [31,32]. It was observed that the total percentage ratio of heat duty transferred by the heat exchangers was 22% and 21% in Case A and B, respectively. This calculation encompasses the heat duty transferred in the heat exchangers

Table 4
Ortho-parahydrogen conversion fraction present along hydrogen streams during liquefaction in both cases.

Case	Case A			Case B		
Component	Hydrogen	Orthohydrogen	Parahydrogen	Hydrogen	Orthohydrogen	Parahydrogen
Stream	**Mole fraction (%)**					
H0	1	0	0	1	–	–
H1	1	0	0	1	–	–
H2	1	0	0	1	–	–
H3	0	0.7410	0.2589	1	–	–
H4	0	0.6909	0.3090	1	–	–
H5	0	0.5234	0.4765	1	–	–
H6	0	0.3912	0.6087	1	–	–
H7	0	0.1618	0.8381	1	–	–
H8	0	0.0632	0.9367	1	–	–
H9	0	0.0395	0.9604	1	–	–
H10	0	0.0264	0.9735	1	–	–
H11	0	0.0220	0.9779	1	–	–

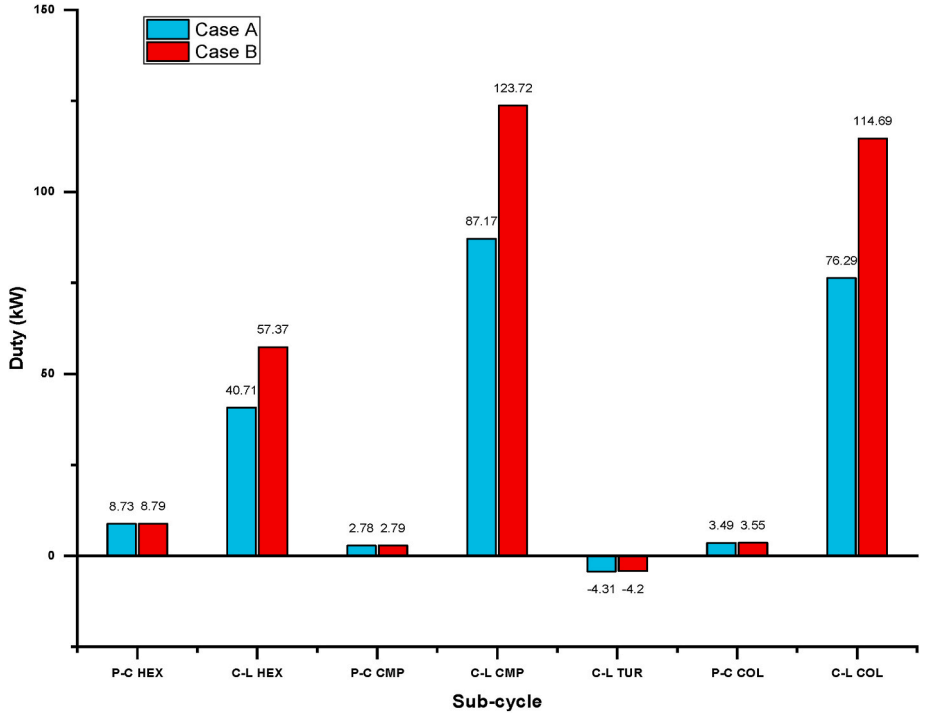

Fig. 5. Duty distribution within the various cycles of the systems: case A – (hydrogen liquefaction with OPHC) and case B – (hydrogen liquefaction without OPHC).

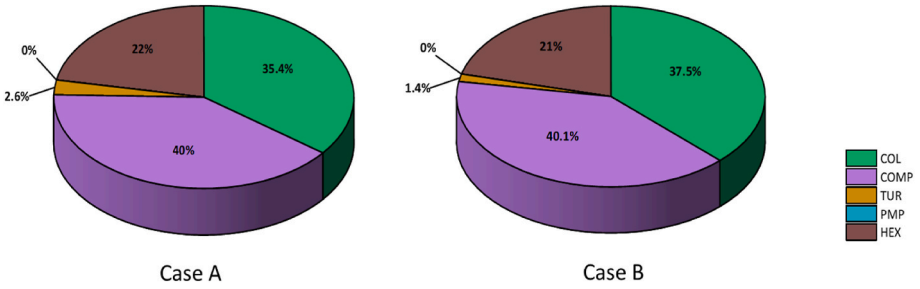

Fig. 6. Comparison of energy consumption and production of major energy-producing and consuming units in the model cases.

during precooling, cooling, and the liquefaction process. The substantial heat transfer percentage observed in the heat exchangers is attributed to the refrigerant absorbing more heat as it undergoes boiling during its transient phase.

The energy generated by the expanders in both cases was relatively minimal. As indicated in Fig. 6, these units contributed only 2.6% and 1.4% to the overall energy of the liquefaction process in both scenarios i.e., case A and B respectively. This limited energy output by the expanders can be ascribed to the extremely low temperatures that the fluids operate under during the liquefaction process. Notably, there was

no difference in the energy output between the expanders in the two cases. This uniformity in energy output between the expanders in both cases can be attributed to the similarity in operational conditions and system configuration within the model.

The consistent operational conditions, such as flow rates, refrigerant properties, compressor efficiencies, and system parameters, likely contributed to the comparable energy consumption. Therefore, factors other than these operational variables, such as specific compressor design characteristics or external factors like system losses, were not significant contributors to the observed energy similarities.

3.2.1. Heat exchangers and ortho-parahydrogen conversion

Heat exchangers were described as the central units of liquefaction for hydrogen. Ortho-parahydrogen conversion was stated to have an effect on the heat exchange units as a result of its heat of conversion during the liquefaction process [9]. With respect to heat transfer, this process is managed by the heat exchangers present in the processes. From Fig. 7, it was observed that Case B exchanged a large amount of duty compared to Case A, respectively. This was likely attributed to high temperatures generated as a result of compression of the refrigerant in the C-L cycle of the Case B model which can be deduced from HX11 and HX13 all located in the refrigerant C-L cycle.

However, the ortho-parahydrogen conversion can be noticed to have less impact on heat exchangers of case A despite being fully integrated into the model case. In fact, it gave more opportunity to find out the orthohydrogen and parahydrogen behaviour as they pass from one heat exchanger to another.

3.3. Exergy analyses

The evaluation of the proposed system involved a thorough analysis of its physical and chemical exergies, exergy destruction, and efficiency. To perform this assessment, a set of equations provided in Table 3 was utilized, and the corresponding results to each stream in the modelled hydrogen liquefaction were tabulated in Table 5.

3.3.1. Exergy destruction

In the case of system performance, Fig. 8 shows the distribution and locations of exergy destruction associated with the hydrogen liquefaction system.

In Case B, from Fig. 8, it has been noted that the compressors have the highest exergy destruction with 173.67 kW for case B compared to case A with just 86.49 kW, followed by the coolers with 45.00 kW in case B as against 33.25 kW of case A as the main sources of exergy losses. Sources like heat exchangers, expanders (turbines), and mixers were minor contributors to exergy losses in the system.

However, for the compressors, major exergy loss was observed in case B because of recycled gaseous hydrogen resulting from partial liquefaction of the hydrogen at the end of the process. This phenomenon produced a boil-off which made the case B process to be more energy demanding as depicted in Fig. 8. Therefore, Case A demonstrated a feature of hydrogen liquefaction efficient process. As for the coolers in both cases, exergy losses can be attributed to the substantial temperature difference between the cooler's inlet and outlet streams. Therefore, the potential energy savings is majorly available in compressors and coolers of the liquefaction system.

Having looked at the variations in the exergy destruction by the various units in the two modelled cases, it has become imperative to find out the cumulative exergy losses by the whole equipment in the models. Fig. 9 shows that the cumulative total exergy destruction by the equipment in case A was 805.34 kW corresponding to 34.1% and 1555.51 kW which is equivalent to 65.9% in Case B.

3.3.2. Exergy efficiency

In the two cases, the precooling section exhibits no significant differences in exergy efficiency. Therefore, the primary focus for detailed comparison lies in evaluating the heat transfer performance within the cooling and liquefaction sections. These sections play critical roles in the overall process, involving further cooling of gases and subsequent conversion to a liquid state. By examining and comparing the exergy efficiencies within these sections, any variations between the two cases can

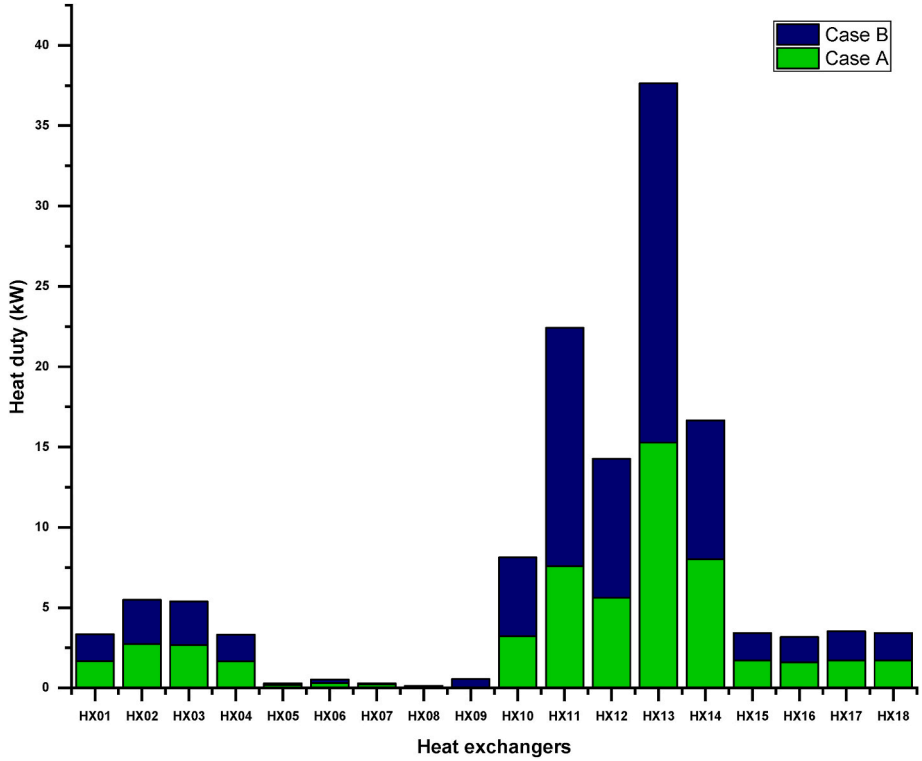

Fig. 7. Effect of ortho-parahydrogen conversion in the heat exchanger's duty.

Table 5
Exergy characteristics of the streams in the designed hydrogen liquefaction structure.

Stream	Physical Exergy (kW)		Chemical Exergy (kW)		Total Exergy (kW)	
	Case A	Case B	Case A	Case B	Case A	Case B
FM1	1.09	1.07	408.27	408.27	409.36	409.34
FM2	0.50	0.50	408.27	408.27	408.77	408.77
FM3	0.47	0.47	380.59	386.32	381.06	386.79
FM4	0.00	0.00	27.71	21.98	27.71	21.98
FM5	1.21	1.22	380.59	386.32	381.80	387.54
FM6	0.00	0.00	27.71	21.98	27.71	21.98
FM7	1.17	1.17	380.59	386.32	381.76	387.49
FM8	1.20	1.20	408.27	408.27	409.47	409.47
FM9	0.01	0.01	53.67	53.29	53.68	53.30
FM10	1.13	1.13	354.66	355.03	355.79	356.17
FM12	1.66	1.66	354.66	355.03	356.32	356.69
FM13	0.01	0.01	53.67	53.29	53.68	53.30
FM14	1.58	1.58	354.66	355.03	356.24	356.61
FM15	1.64	1.64	408.27	408.27	409.91	409.91
FM16	1.43	1.43	273.35	273.34	274.78	274.77
FM17	0.09	0.09	135.05	135.06	135.13	135.15
FM18	1.60	1.60	273.35	273.34	274.95	274.94
FM19	0.12	0.12	135.05	135.06	135.17	135.18
FM20	1.12	1.12	145.04	145.04	146.15	146.16
FM21	0.35	0.35	128.45	128.44	128.81	128.79
FM22	1.91	1.91	145.04	145.04	146.94	146.94
FM23	0.32	0.32	135.05	135.06	135.37	135.38
FM24	2.96	2.96	145.04	145.04	147.99	147.99
FM25	0.64	0.64	135.05	135.06	135.69	135.70
FM26	3.56	3.56	408.27	408.27	411.83	411.83
FM27	3.30	3.30	408.27	408.27	411.57	411.57
FM28	5.98	5.98	408.27	408.27	414.25	414.25
FM29	2.89	2.89	408.27	408.27	411.16	411.16
FM30	0.31	0.31	30.76	30.72	31.07	31.03
FM31	2.30	2.30	377.80	377.84	380.09	380.13
FM32	0.17	0.17	30.76	30.72	30.94	30.90
FM33	0.81	0.80	377.80	377.84	378.61	378.63
H0	0.96	0.95	65.58	65.58	66.54	66.54
H1	2.57	2.57	65.58	65.58	68.15	68.15
H2	2.11	2.10	65.58	65.58	67.69	67.68
H3	2.18	2.18	−0.39	65.58	1.78	67.76
H4	2.57	2.60	−0.43	65.58	2.14	68.18
H5	3.46	3.47	−0.48	65.58	2.99	69.05
H6	4.10	4.16	−0.46	78.60	3.64	82.76
H7	5.53	4.42	−0.30	78.60	5.22	83.02
H8	7.07	5.20	−0.16	78.60	6.90	83.81
H9	7.56	5.51	−0.11	78.60	7.45	84.11
H10	7.88	5.91	−0.08	78.60	7.80	84.51
H11	7.70	9.09	−0.07	78.60	7.63	87.69
H12	a	8.97	a	78.60	a	87.57
H13	a	8.20	a	65.58	a	73.78
H14	a	0.68	a	13.02	a	13.70
H15	a	0.67	a	13.02	a	13.69
SM1	11.37	14.74	191.59	248.42	202.96	263.16
SM2	1.14	1.47	19.16	24.84	20.30	26.32
SM3	2.27	3.68	38.32	62.11	40.59	65.79
SM4	1.71	2.21	28.74	37.26	30.44	39.47
SM5	3.98	5.16	67.06	86.95	71.04	92.11
SM6	2.27	2.21	38.32	37.26	40.59	39.47
SM7	8.50	11.02	19.16	24.84	27.66	35.86
SM8	5.52	7.16	19.16	24.84	24.68	32.00
SM9	6.56	8.93	19.16	24.84	25.72	33.77
SM10	3.71	5.40	19.16	24.84	22.87	30.24
SM11	2.92	4.93	19.16	24.84	22.08	29.77
SM12	0.00	0.00	19.16	24.84	19.16	24.84
SM13	7.83	10.15	19.16	24.84	26.99	34.99
SM14	5.68	9.21	38.32	62.11	44.00	71.31
SM15	5.33	8.81	38.32	62.11	43.65	70.92
SM16	11.05	17.91	38.32	62.11	49.37	80.02
SM17	9.00	14.59	38.32	62.11	47.32	76.70
SM18	7.39	13.37	38.32	62.11	45.70	75.47
SM19	0.05	0.17	38.32	62.11	38.36	62.27
SM20	10.11	17.38	38.32	62.11	48.42	79.49
SM21	4.26	5.52	28.74	37.26	33.00	42.79
SM22	3.96	5.19	28.74	37.26	32.70	42.45
SM23	9.18	11.90	28.74	37.26	37.91	49.16
SM24	7.01	9.09	28.74	37.26	35.75	46.36
SM25	5.26	8.55	28.74	37.26	34.00	45.81
SM26	−1.68	−2.16	28.74	37.26	27.06	35.10
SM27	5.25	7.08	28.74	37.26	33.99	44.34
SM28	9.94	12.89	67.06	86.95	77.00	99.84
SM29	9.54	12.45	67.06	86.95	76.60	99.40
SM30	22.28	28.89	67.06	86.95	89.34	115.83
SM31	14.59	18.91	67.06	86.95	81.64	105.86
SM32	13.97	18.19	67.06	86.95	81.02	105.14
SM33	−6.67	−8.59	67.06	86.95	60.39	78.36
SM34	19.33	25.73	67.06	86.95	86.39	112.67
SM35	5.68	5.52	38.32	37.26	44.00	42.79
SM36	5.33	5.18	38.32	37.26	43.65	42.44
SM37	12.73	12.38	38.32	37.26	51.05	49.64
SM38	9.74	9.48	38.32	37.26	48.06	46.74
SM39	9.30	4.97	38.32	37.26	47.62	42.23
SM40	−3.90	−3.76	38.32	37.26	34.42	33.51
SM41	6.21	6.59	38.32	37.26	44.52	43.85
SM42	38.84	53.08	191.59	248.42	230.43	301.50
W1	0.00	0.00	2.64	2.64	2.64	2.64
W2	0.19	0.19	2.64	2.64	2.82	2.82
W3	0.00	0.00	2.64	2.64	2.64	2.64
W4	0.16	0.16	2.64	2.64	2.80	2.80
W5	0.00	0.00	2.64	2.64	2.64	2.64
W6	0.14	0.14	2.64	2.64	2.78	2.78
W7	0.00	0.00	2.64	2.64	2.64	2.64
W8	0.16	0.18	2.64	2.64	2.80	2.82
W9	0.00	0.00	2.64	2.64	2.64	2.64
W10	0.16	0.16	2.64	2.64	2.80	2.80

[a] Streams not applicable in the Case model.

be assessed. This targeted analysis allows for the optimal processes in the cooling and liquefaction sections, potentially leading to improved overall efficiency and effectiveness of the hydrogen liquefaction system. Table 6 shows the exergy efficiency and exergy destruction rate of the equipment.

3.3.2.1. Compressors. From Table 6, it is obvious that the compressors were efficient with respect to exergy destruction as it was shown that almost all of them achieved an average exergy efficiency higher than 90% in both cases. The rise in average exergy efficiencies in both cases was because of the absence of H_2 in the fluid component mixture of the second MR cycle which would have consumed a considerable amount of energy for its compression because of its low molecular weight. On the other hand, in case B, the compressors exhibited lower exergy efficiency compared to case A due to the recycled boil-off hydrogen. This reintroduction of boil-off hydrogen at a lower pressure is needed to be pressurised again for reliquefication. In doing so, the temperature of the hydrogen is increased adding more heat load to the system thereby reducing the efficiency of compressors in case B.

3.3.2.2. Coolers. The coolers, predominantly located in the pre-cooling sections of the liquefaction process, exhibited high average exergy efficiencies of 95.45% and 95.29% for cases A and B respectively. This was attributed to the small temperature difference between the inlet and outlet streams of the coolers.

3.3.2.3. Heat exchangers. Heat exchangers are integral components within the hydrogen liquefaction system, representing the equipment with the highest proportion. They play a crucial role in facilitating heat transfer processes, enabling efficient cooling of hydrogen gas. Due to the high energy requirements and temperature differentials involved in the liquefaction process, heat exchangers are essential for achieving the desired low temperatures and optimal system performance. In the proposed setup, a total of eighteen heat exchangers are utilized. According to Table 6, the heat exchangers in both cases A and B have an average exergy efficiency of 98.78% and 98.68% respectively. However, the heat

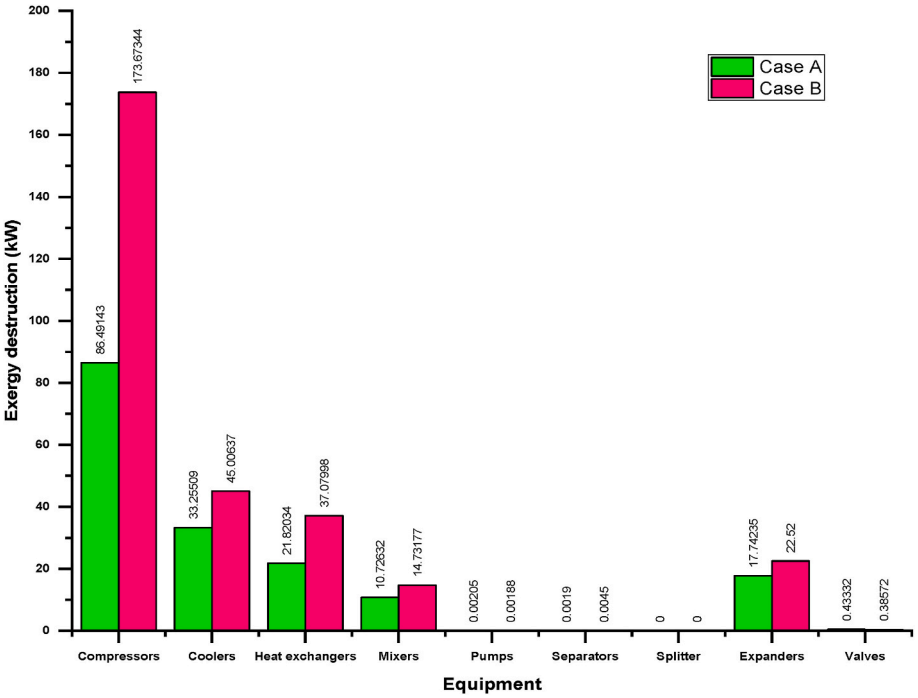

Fig. 8. Comparison of exergy destruction in major equipment of model cases.

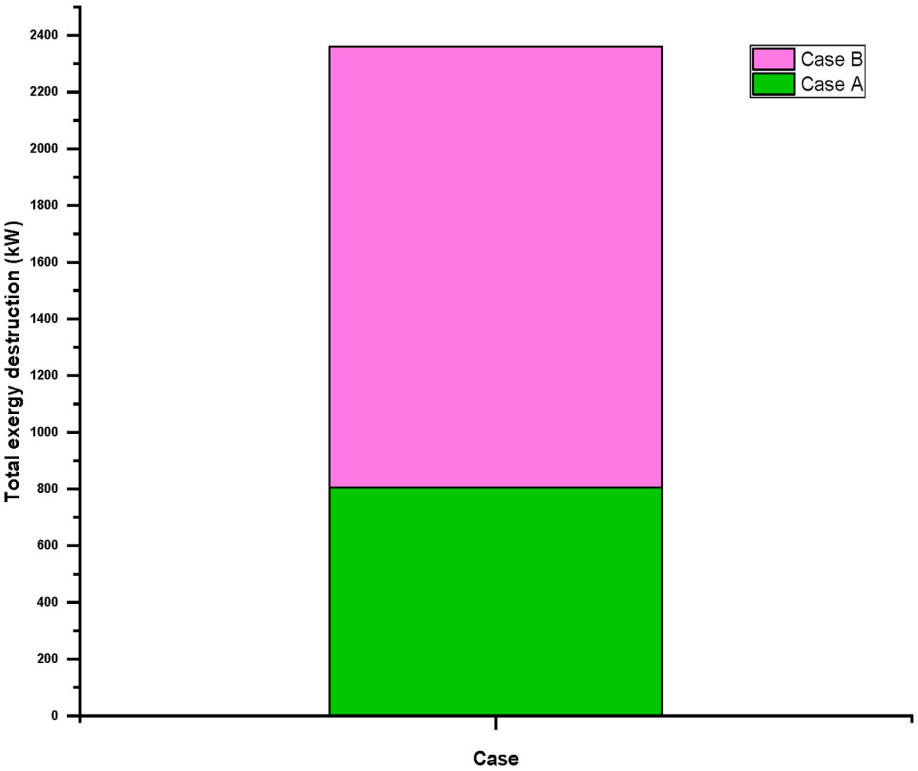

Fig. 9. Comparison of cumulative total exergy destruction in the two systems.

exchangers in the designed models (HX03 for case A and HX02, HX03 for case B) had the highest efficiencies of 99.96% and 99.97% among other units respectively.

3.3.2.4. Expanders. Expanders, all located in the second refrigeration cycles of the models, have an average exergy efficiency (92.92% and 92.96%) in cases A and B respectively than other equipment.

3.3.2.5. Pumps. Table 6 indicated a significant decrease in the exergy efficiency of the pumps in the designed hydrogen liquefaction systems averaging 25.97% and 23.49% in cases A and B respectively. The reason for this phenomenon is that at lower temperatures, entropy generation has a lower value [33].

Table 6
Exergy efficiency of the equipment in the two modelled hydrogen liquefaction systems.

Equipment	Average Exergy Efficiency (%)	
	Case A	Case B
Compressors	92.64	90.43
Coolers	95.45	95.29
Heat Exchangers	98.71	98.68
Mixers	99.13	99.13
Pumps	25.97	23.49
Separators	100.00	99.99
Splitters	100.00	99.99
Expanders	92.92	92.96
Valve	99.89	99.13

3.4. Specific energy consumption

To evaluate the performance of the hydrogen liquefaction process, the two cases, A and B were considered, in relation to their specific energy consumption (SEC) and coefficient of performance (COP). All parameters were kept constant irrespective of either case to ensure a smooth comparison, and the results were tabulated in Table 7.

The comparison revealed that, at the same refrigerant mass flow rate, case A, which incorporates continuous operation of OPHC, exhibited a lower SEC value of 8.45 kWh/kg_{LH}. In contrast, case B demonstrated a higher SEC value of 15.65 kWh/kg_{LH}. These values indicate the amount of energy consumed per unit of hydrogen liquefied for each case.

To assess the performance potential of the hydrogen liquefaction process further, a coefficient of performance (COP) analysis was conducted on the hydrogen liquefaction system. This analysis is to shed light on the amount of heat that must be transferred during each process to evaluate the system's efficiency in converting input energy into hydrogen liquefaction [33,34]. By calculating the COP values for different cases, one can determine the heat transfer requirements for each specific scenario. In the obtained results, the COP values for both cases (A and B) were determined to be 0.0371 and 0.0218 respectively. This low value suggests that a relatively high amount of energy needs to be transferred in order to achieve hydrogen liquefaction in all the modelled cases, making it a more energy-inefficient process.

3.5. Boil-off analysis

Boil-off, the evaporation of a portion of liquid hydrogen, is linked to process inefficiencies and energy losses. To enhance the viability and competitiveness of liquid hydrogen storage, it is imperative to minimize boil-off or, as an alternative, recover and reliquify the gaseous hydrogen. This process of recovery adds a huge cost effect on the hydrogen liquefaction process [35,36].

From Table 8 it can be seen that at the liquefaction stage boiloff occurred in case B reducing the liquefied hydrogen temperature from −245 °C to −242.31 °C. This made it necessary to recover the boiloff and recycle it for reliquefaction thereby increasing the inefficiency of the system. However, on the other hand, case A shows a smooth liquefaction process without significant boiloff [37,38]. This is further demonstrated by the SEC results in Table 7.

According to the results presented in Table 9, case A showed no evidence of hydrogen evaporation, suggesting that the liquefaction process was fully successful. This successful outcome can be attributed to the presence of the catalysed OPHC process facilitating the liquefaction. Conversely, in case B, approximately 19.85% of the hydrogen feed for liquefaction evaporated. This evaporation indicates a boil-off in the liquefaction process, resulting from the absence of a catalysed OPHC process.

Table 7
SEC and COP analysis of the two modelled hydrogen liquefaction cases.

Model	System Exergy Efficiency	SEC [kWhr/kg_{LH}]	COP
Case A	92.42	8.45	0.0371
Case B	87.18	15.65	0.0218

Table 8
Temperature of the hydrogen streams indicating boil-off during liquefaction process in the hydrogen liquefaction system of the two cases.

Stream	Cycle	Pressure (bar)	Temperature (°C)		Remarks
			Case A	Case B	
H0	Compression	4	25.00	25.00	
H1		21	250.72	250.72	
H2	Precooling	21	45.00	45.00	
H3		21	−45.00	−45.00	
H4		21	−130.00	−130.00	
H5		21	−192.00	−192.00	
H6		21	−210.00	−191.28	
H7	Cryogenic cooling	21	−230.00	−200.00	
H8		21	−239.00	−220.00	
H9		21	−242.00	−225.00	
H10		21	−244.13	−230.00	
H11	Liquefaction	1	−245.99	−245.00	
H12		1	[a]	−242.31	Boiloff observed in Case B
H13	Recycle	1	[a]	−245.31	
H14		1	[a]	−245.31	
H15		21	[a]	−187.35	

[a] Streams not applicable in the Case model.

4. Conclusion, future perspectives and research directions

A comprehensive comparative analysis of two hydrogen liquefaction systems (OPHC and non-OPHC systems) was studied with the aim of analysing the effect of orthohydrogen to parahydrogen conversion on hydrogen liquefaction. The Brayton cycle and Peng-Robinson equation of state were used for the process design and simulation. Two mixed refrigerants were used for both the precooling and cryogenic cooling cycles in the liquefaction.

Impact of OPHC on energy consumption, energy and exergy efficiencies, and exergy destruction were evaluated with the following major findings:

- The sub-cycles energy analysis revealed that the compressors and coolers consumed the highest energy in both cases with case B having larger consumption compared to case A.
- The cryogenic heat exchangers transferred larger amounts of duty compared to the heat exchangers in precooling in both cases.
- Exergy efficiencies of the two cases (A and B) were calculated to be 92.42% and 87.18% respectively with case B having the highest value of exergy destruction compared to case A.
- Exergy destruction was observed to have occurred largely in the compressors and coolers in both cases.
- The calculated SEC value for case A and B were 8.45 kWhr/kg_{LH} and 15.65 kW/kg_{LH} respectively.
- In the total liquefaction process, the COP of both cases (A and B) was calculated to be 0.0371 and 0.0218 respectively.

Table 9
Amount of hydrogen evaporated.

Parameter	Evaporated amount (%)	
Case	Case A	Case B
Component		
Hydrogen	–	19.85

It can be concluded that case A process is more favourable compared to case B. Therefore, adopting catalysed OPHC technology offers notable advantages in terms of energy consumption and exergy efficiency. It is recommended that future study should explore novel catalyst materials for OPHC, mixed refrigerants and optimize the liquefaction process of both cases.

CRediT authorship contribution statement

Abdurrazzaq Ahmad: Writing – review & editing, Writing – original draft, Visualization, Validation, Software, Methodology, Funding acquisition, Formal analysis, Data curation, Conceptualization. **Eni Oko:** Writing – review & editing, Writing – original draft, Supervision, Software, Project administration, Methodology, Funding acquisition, Conceptualization. **Alex Ibhadon:** Writing – review & editing, Supervision, Funding acquisition.

Declaration of competing interest

The authors declare the following financial interests/personal relationships which may be considered as potential competing interests:

Abdurrazzaq Ahmad reports financial support was provided by Tertiary Education Trust Fund. Eni Oko reports financial support was provided by Engineering and Physical Sciences Research Council. If there are other authors, they declare that they have no known competing financial interests or personal relationships that could have appeared to influence the work reported in this paper.

Acknowledgement

The authors are grateful to Tertiary Education Trust Fund Nigeria and the Engineering and Physical Science Research (EPSRC)/Industrial Decarbonisation Research & Innovation Centre (IDRIC) Flexible Funding Round 4 for financially supporting this project. The authors are wholly responsible for the contents of this paper.

Appendix A. Supplementary data

Supplementary data to this article can be found online at https://doi.org/10.1016/j.ijhydene.2024.06.368.

References

[1] Ghorbani B, Mehrpooya M, Aasadnia M, Niasar MS. Hydrogen liquefaction process using solar energy and organic Rankine cycle power system. J Clean Prod 2019; 235:1465–82. https://doi.org/10.1016/j.jclepro.2019.06.227.
[2] Hartl M, Gillis RC, Daemen L, Olds DP, Page K, Carlson S, et al. Hydrogen adsorption on two catalysts for the ortho- to parahydrogen conversion: Cr-doped silica and ferric oxide gel. Phys Chem Chem Phys 2016;18:17281–93. https://doi.org/10.1039/c6cp01154c.
[3] Zheng J, Liu X, Xu P, Liu P, Zhao Y, Yang J. Development of high pressure gaseous hydrogen storage technologies. Int J Hydrogen Energy 2012;37:1048–57. https://doi.org/10.1016/j.ijhydene.2011.02.125.
[4] Al Ghafri SZ, Munro S, Cardella U, Funke T, Notardonato W, Trusler JPM, et al. Hydrogen liquefaction: a review of the fundamental physics, engineering practice and future opportunities. Energy Environ Sci 2022;15:2690–731. https://doi.org/10.1039/d2ee00099g.
[5] Rusman NAA, Dahari M. A review on the current progress of metal hydrides material for solid-state hydrogen storage applications. Int J Hydrogen Energy 2016; 41:12108–26. https://doi.org/10.1016/j.ijhydene.2016.05.244.
[6] Cardella U, Decker L, Klein H. Roadmap to economically viable hydrogen liquefaction. Int J Hydrogen Energy 2017;42:13329–38. https://doi.org/10.1016/j.ijhydene.2017.01.068.
[7] Leachman JW, Jacobsen RT, Penoncello SG, Lemmon EW. Fundamental equations of state for parahydrogen, normal hydrogen, and orthohydrogen. J Phys Chem Ref Data 2009;38:721–48. https://doi.org/10.1063/1.3160306.
[8] Pingkuo L, Xue H. Comparative analysis on similarities and differences of hydrogen energy development in the World's top 4 largest economies: a novel framework. Int J Hydrogen Energy 2022;47:9485–503. https://doi.org/10.1016/j.ijhydene.2022.01.038.
[9] Riaz A, Qyyum MA, Hussain A, Lee M. Significance of ortho-para hydrogen conversion in the performance of hydrogen liquefaction process. Int J Hydrogen Energy 2022. https://doi.org/10.1016/j.ijhydene.2022.09.022.
[10] Son H, Yu T, Hwang J, Lim Y. Simulation methodology for hydrogen liquefaction process design considering hydrogen characteristics. Int J Hydrogen Energy 2022; 47:25662–78. https://doi.org/10.1016/j.ijhydene.2022.05.293.
[11] Bi Y, Ju Y. Design and analysis of an efficient hydrogen liquefaction process based on helium reverse Brayton cycle integrating with steam methane reforming and liquefied natural gas cold energy utilization. Energy 2022;252. https://doi.org/10.1016/j.energy.2022.124047.
[12] Yuksel YE, Ozturk M, Dincer I. Analysis and assessment of a novel hydrogen liquefaction process. Int J Hydrogen Energy 2017;42:11429–38. https://doi.org/10.1016/j.ijhydene.2017.03.064.
[13] Teng J, Wang K, Zhu S, Bao S, Zhi X, Zhang X, et al. Comparative study on thermodynamic performance of hydrogen liquefaction processes with various ortho-para hydrogen conversion methods. Energy 2023;271. https://doi.org/10.1016/j.energy.2023.127016.
[14] Farkas A, Farkas L, Harteck P. Experiments on heavy hydrogen. II. The ortho-para conversion, 144; 1934.
[15] Qyyum MA, Riaz A, Naquash A, Haider J, Qadeer K, Nawaz A, et al. 100% saturated liquid hydrogen production: mixed-refrigerant cascaded process with two-stage ortho-to-para hydrogen conversion. Energy Convers Manag 2021;246. https://doi.org/10.1016/j.enconman.2021.114659.
[16] Zhou H, Li Z, Li M, He M, Wu Q, Gong L. Study of activation methods for Ortho-para hydrogen catalysts in a small isothermal converter based on gas chromatography at LN2 temperature. Int J Hydrogen Energy 2024;55:55–64. https://doi.org/10.1016/j.ijhydene.2023.10.155.
[17] Saghatoleslami N, Sargolzaie J. Design of the reactor, selection of catalyst for ortho to para hydrogen conversion and preliminary design of cryogenic system for its liquefaction. J Chem & Chem Eng 2004;23:4.
[18] Yang M, Hunger R, Berrettoni S, Sprecher B, Wang B. A review of hydrogen storage and transport technologies. Clean Energy 2023;7:190–216. https://doi.org/10.1093/ce/zkad021.
[19] Alekseev A. Hydrogen science and engineering: materials, processes, systems and technology. In: Stolten Detlef, Emonts Bernd, editors. Hydrogen science and engineering: materials, processes, systems and technology. First. Wiley-VCH Verlag GmbH & Co. KGaA; 2016. p. 733–61.
[20] Lv C, Zhou G, Wang J, He M, Wu J, Gong L. Design method of the hydrogen liquefaction process with catalyst-filled heat exchanger model. Springer Proc Phys 2024;393:132–40. https://doi.org/10.1007/978-981-99-8631-6_15. Springer Science and Business Media Deutschland GmbH.
[21] Teng J, Wang K, Zhu S, Bao S, Zhi X, Zhang X, et al. Comparative study on thermodynamic performance of hydrogen liquefaction processes with various ortho-para hydrogen conversion methods. Energy 2023;271. https://doi.org/10.1016/j.energy.2023.127016.
[22] Nouri M, Miansari M, Ghorbani B. Exergy and economic analyses of a novel hybrid structure for simultaneous production of liquid hydrogen and carbon dioxide using photovoltaic and electrolyzer systems. J Clean Prod 2020;259. https://doi.org/10.1016/j.jclepro.2020.120862.
[23] Ohira K. A summary of liquid hydrogen and cryogenic technologies in Japan's WE-NET Project. AIP Conf Proc 2004;710:27–34. https://doi.org/10.1063/1.1774663. American Institute of Physics Inc.
[24] Bi Y, Yin L, He T, Ju Y. Optimization and analysis of a novel hydrogen liquefaction process for circulating hydrogen refrigeration. Int J Hydrogen Energy 2022;47: 348–64. https://doi.org/10.1016/j.ijhydene.2021.10.012.
[25] Hammad A, Dincer I. Analysis and assessment of an advanced hydrogen liquefaction system. Int J Hydrogen Energy 2018;43:1139–51. https://doi.org/10.1016/j.ijhydene.2017.10.158.
[26] Lee H, Haider J, Abdul Qyyum M, Choe C, Lim H. An innovative high energy efficiency–based process enhancement of hydrogen liquefaction: energy, exergy, and economic perspectives. Fuel 2022;320. https://doi.org/10.1016/j.fuel.2022.123964.
[27] Sadaghiani MS, Mehrpooya M. Introducing and energy analysis of a novel cryogenic hydrogen liquefaction process configuration. Int J Hydrogen Energy 2017;42:6033–50. https://doi.org/10.1016/j.ijhydene.2017.01.136.
[28] Asadnia M, Mehrpooya M. A novel hydrogen liquefaction process configuration with combined mixed refrigerant systems. Int J Hydrogen Energy 2017;42: 15564–85. https://doi.org/10.1016/j.ijhydene.2017.04.260.
[29] Riaz A, Qyyum MA, Min S, Lee S, Lee M. Performance improvement potential of harnessing LNG regasification for hydrogen liquefaction process: energy and exergy perspectives. Appl Energy 2021;301. https://doi.org/10.1016/j.apenergy.2021.117471.
[30] Naquash A, Riaz A, Lee H, Qyyum MA, Lee S, Lam SS, et al. Hydrofluoroolefin-based mixed refrigerant for enhanced performance of hydrogen liquefaction process. Int J Hydrogen Energy 2022;47:41648–62. https://doi.org/10.1016/j.ijhydene.2022.02.010.
[31] Aasadnia M, Mehrpooya M. Large-scale liquid hydrogen production methods and approaches: a review. Appl Energy 2018;212:57–83. https://doi.org/10.1016/j.apenergy.2017.12.033.
[32] Park S, Noh W, Park J, Park J, Lee I. Efficient heat exchange configuration for sub-cooling cycle of hydrogen liquefaction process. Energies 2022;15. https://doi.org/10.3390/en15134560.
[33] Yin L, Ju Y. Review on the design and optimization of hydrogen liquefaction processes. Front Energy 2020;14:530–44. https://doi.org/10.1007/s11708-019-0657-4.
[34] Yin L, Ju Y. Process optimization and analysis of a novel hydrogen liquefaction cycle. Int J Refrig 2020;110:219–30. https://doi.org/10.1016/j.ijrefrig.2019.11.004.

[35] Morales-Ospino R, Celzard A, Fierro V. Strategies to recover and minimize boil-off losses during liquid hydrogen storage. Renew Sustain Energy Rev 2023;182. https://doi.org/10.1016/j.rser.2023.113360.
[36] Riaz A, Qyyum MA, Hussain A, Lee M. Significance of ortho-para hydrogen conversion in the performance of hydrogen liquefaction process. Int J Hydrogen Energy 2023;48:26568–82. https://doi.org/10.1016/j.ijhydene.2022.09.022.
[37] Qyyum MA, Riaz A, Naquash A, Haider J, Qadeer K, Nawaz A, et al. 100% saturated liquid hydrogen production: mixed-refrigerant cascaded process with two-stage ortho-to-para hydrogen conversion. Energy Convers Manag 2021;246. https://doi.org/10.1016/j.enconman.2021.114659.
[38] Krasae-in S, Stang JH, Neksa P. Development of large-scale hydrogen liquefaction processes from 1898 to 2009. Int J Hydrogen Energy 2010;35:4524–33. https://doi.org/10.1016/j.ijhydene.2010.02.109.